Journal of Thermal Science Vol.33, No.5 (2024) 1974–1989

https://doi.org/10.1007/s11630-024-2022-0 **Article ID: 1003-2169(2024)05-1974-16**

Effect of Operation Parameters on the Thermal Characteristics in a Planar Solid Oxide Fuel Cell

WANG Mingyuan[1,2], WANG Ke[1,2*], WANG Yongqing[2,3], CHEN Jiangshuai[2,3], AN Bo[1,2], TU Shantung[2,4]

1. School of Mechanics and Safety Engineering, Zhengzhou University, Zhengzhou 450001, China
2. Key Laboratory of Process Heat Transfer and Energy Saving of Henan Province, Zhengzhou University, Zhengzhou 450002, China
3. School of Mechanical and Power Engineering, Zhengzhou University, Zhengzhou 450001, China
4. Key Laboratory of Pressure Systems and Safety (MOE), East China University of Science & Technology, Shanghai 200237, China

Abstract: Effective operation strategies in the solid oxide fuel cell (SOFC) can adjust the spatial distribution of temperature gradient favoring the long-term stability. To investigate the effects of different operating conditions on the thermal behavior inside SOFC, a three-dimensional model is developed in this study. The model is verified by comparing it with the experimental data. The heat generation rate and its variation under different operating conditions are analyzed. The combined effects of operating voltage and gas temperature are considered to be the key factor influencing the temperature gradient. Compared to the original case, the temperature of SOFC decreases by 21.4 K when the fuel velocity reaches 5 m/s. But the maximum temperature gradient increases by 21.2%. Meanwhile, higher fuel velocities can eliminate about 32% of the area with higher temperature gradient. And when the oxidant velocity reaches 7.5 m/s, the peak temperature gradient effectively decreases by 16.59%. Simultaneous adjustment of the oxidant and fuel velocities can effectively reduce the peak temperature gradient and increase the safety zone. The effects of operation conditions on the temperature gradient of the cell are clarified in this study, which can be a reference for further research on the reliability of SOFCs.

Keywords: SOFC; heat generation; temperature gradient distribution; heat source; thermal behavior

1. Introduction

Solid oxide fuel cell (SOFC) is an energy conversion device with high efficiency. The efficiency of SOFC is not limited by the Carnot Cycle, and it is a new energy device attracting many scholars' interests [1]. In SOFC, it is allowed to use various types of fuels. A high operating temperature allows direct reforming of the fuel gas at the anode, and the exhausted gas is environmentally friendly water vapor or carbon dioxide [2, 3]. These advantages make SOFC widely used in various fields of distributed power generation. Among them, the planar SOFC is simple to manufacture and flexible in cell geometry and gas manifold stacking [4].

Received: Jul 26, 2023 AE: LI Yinshi Corresponding author: WANG Ke E-mail: kewang@zzu.edu.cn

SOFCs operate at high temperatures and have significant thermodynamic and kinetic advantages. Its performance is affected by many factors, including operation conditions [5, 6], microstructural parameters [7, 8], flow field design [9, 10], and component material [11]. However, thermal management is a major challenge due to the high temperature operation environment. Higher power density leads to a bigger temperature gradient in the SOFC due to local heat generation and uneven heat dissipation [12]. Meanwhile the mismatch of the coefficients of thermal expansion (CTEs) of different components generates great thermal stress [13, 14], which leads to cracks in SOFC [15, 16], or even failure [17, 18]. Inhomogeneous temperature distributions are often observed in SOFC assemblies or stacks, especially in internally reformed SOFCs [19, 20], posing a threat to material deterioration and structural integrity. Therefore, clarifying the temperature gradient distribution and heat transfer mechanisms within SOFCs during operation is crucial for the effective lifetime management of the device.

The temperature uniformity and concentration distribution of SOFC are affected by its electrochemical and thermal characteristics [21]. Some scholars made the gas concentration distribution in SOFC more uniform to improve the uniformity of temperature distribution by changing the structures of the flow channels [22, 23], or by changing the flow distribution [24, 25]. Flow patterns provide non-uniform heat transfer paths, which also make the non-uniform temperature distribution. Zhang et al. [26] compared the SOFC performance of three flow modes and found that the temperatures of the three flow arrangements distribute non-uniformly. Choudhary et al. [27] compared the performances of SOFCs with the modes of co-flow and counter-flow, and found that the counter-flow mode shows better performance in current and power densities. However, SOFCs with counter-flow mode are of steep temperature gradients in the PEN structure.

The thermal balance between the conduction of metal interconnects, gas convection, and heat generated by electrochemical reactions determines the temperature gradient along the cell and its distribution [28]. Advection through the stacks and metal conduction between repeating units may change the heat transfer path and internal thermal conditions [29]. Effective thermal management methods are necessary to reduce the temperature gradient in SOFCs. Zheng et al. [30] proposed a novel cooler for thermal management in the SOFC stacks by controlling precisely the endothermic ammonia cracking reaction in the cooler. Zeng et al. [31] added turbulators inside the air flow channel of the tubular SOFC. By inducing the recirculation flow, the local convective heat transfer coefficient was increased, which effectively reduced the maximum temperature gradient. In addition to the above methods, excessive internal temperature gradients can also be reduced by introducing excess air [32, 33] or changing the thermal conductivity of the material [34]. However, although the thermal behavior of SOFCs has been extensively studied, two-dimensional models were used and the interconnector was not considered in most of the previous studies [35, 36]. Besides, few studies have focused on the quantitative relationship between operation conditions and temperature gradient. Zeng et al. [31] have reported that a spatial temperature gradient diagram helps to understand the temperature gradient distribution. Inspired by the above work, this study uses this diagram to analyze the relationship between operation conditions and temperature gradient.

In the manuscript, a 3D numerical model was constructed to analyze the relationship between different operation conditions and thermal characteristics. The generation and consumption of species, electrochemical reactions, and the generation and transfer of heat are fully considered. This study focuses on the thermal characteristics of SOFCs under different operating conditions, especially the spatial distribution of the temperature gradient under different operating conditions. In addition, this study focuses on the quantitative relationship between heat generation rate and heat transfer rate under different operation conditions. The results of this study help to understand deeply the thermal management of SOFC, which is important for the reliability of SOFC during operation.

2. SOFC Modeling

2.1 Physical model

In practice, the planar SOFC generally operates as a stack. The stack is composed of multiple single-layer cells stacked repeatedly. Each cell contains a dense electrolyte and porous electrodes. Gas channels are formed through metal interconnects, and the transfer of electrons and heat is completed by the interconnects [28, 37]. Due to the repetitive characteristics inside the stack and the symmetric structure and physical field of each cell, only the simplest cell is modeled and analyzed. A model for a planar anode-supported SOFC is developed using COMSOL MULTIPHYSICS. The computational domain of the cell is shown in Fig. 1(a), which comprises metal interconnectors, gas channels, an anode of Ni-YSZ, an electrolyte of YSZ, and a cathode of LSM-YSZ.

The geometric parameters of the physical model are shown in Table 1, which are corresponding to Ref. [38, 39]. The oxidant and fuel are regarded as ideal gases, and the flow is laminar due to the low Reynolds number (< 2000) in the numerical calculation. The reactant in the

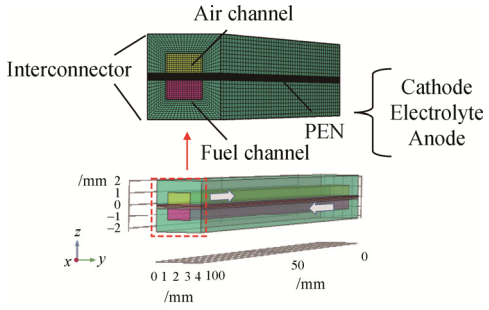

(a) Computational domain

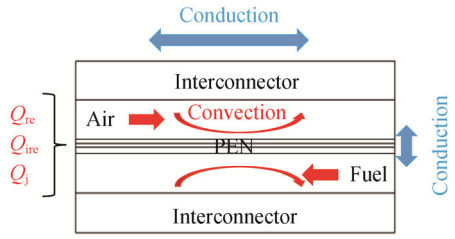

(b) Heat generation and transfer

Fig. 1 Numerical model

Table 1 SOFC geometric parameters [38, 39]

Parameter	Value	Unit
Cathode thickness [38, 39]	100	μm
Anode thickness [38, 39]	150	μm
Electrolyte thickness [38, 39]	100	μm
Gas channel width [38, 39]	2	mm
Gas channel height [38, 39]	1	mm
Interconnect height [38, 39]	2	mm
Cell length [38, 39]	100	mm

gas channels flows in the counter direction. Thermal conduction and convective heat transfer are considered, while radiation heat transfer is ignored [40]. Contact thermal resistances between electrodes and interconnects are ignored.

2.2 Governing equations

SOFC in actual operation involves a number of complex physicochemical processes such as the flow of reacting gases inside the flow channel, diffusion in the porous electrodes, electrochemical reactions in the reaction region, and heat transfer. These physical fields are coupled to each other and together they affect the output performance of SOFCs. In our previous study [41], some governing equations are used for calculation and solution. The governing equations are listed in Table 2.

2.3 Boundary conditions and operation parameters

Table 3 lists some operation parameters in this study, which is corresponding to that in Refs. [38, 39]. The voltages on the upper surface of the cathode-side interconnect are set to the operating voltage, and the lower surface of the anode-side interconnect is set as the ground potential. Then some parameters are varied to explore their effects on thermal behavior. The detailed boundary conditions are summarized in Table 4.

2.4 Model validation

The mesh numbers of 39 000, 60 000, 88 000, 100 800 are selected to verify the grid dependence under this calculation. According to Table 5, the current density difference with the further increased gird is less than 0.5%. Therefore, Mesh3 (88 000) meshing method is

Table 2 Governing equations [42–44]

	Governing equations
Charge conservation	$\nabla\cdot i_{el}=\nabla\cdot\left(-\sigma_{el}^{eff}\nabla\varphi_{el}\right)=Q_{el},\ \nabla\cdot i_{io}=\nabla\cdot\left(-\sigma_{io}^{eff}\nabla\varphi_{io}\right)=Q_{io}$
Electrochemical model	$i_a=i_{0,a}S_V\left[\frac{C_{H_2}}{C_{H_2,ref}}\exp\left(\frac{\alpha_a^a F\eta_{act,a}}{RT}\right)-\frac{C_{H_2O}}{C_{H_2O,ref}}\exp\left(\frac{-\alpha_c^a F\eta_{act,a}}{RT}\right)\right]$
	$i_c=i_{0,c}S_V\left[\exp\left(\frac{\alpha_a^c F\eta_{act,c}}{RT}\right)-\frac{C_{O_2}}{C_{O_2,ref}}\exp\left(\frac{-\alpha_c^c F\eta_{act,c}}{RT}\right)\right]$
Mass and momentum conservation	$\nabla\cdot(\rho\vec{u})=Q_{br}$
	$\frac{\rho}{\varepsilon}(\vec{u}\cdot\nabla)\vec{u}=-\varepsilon\nabla p+\nabla\left[\mu\left(\psi-\frac{2}{3}\nabla\cdot\vec{u}\right)\right]+\varepsilon\vec{F}$
Species conservation	$\nabla\cdot\left\{\omega_i\rho u-\rho\omega_i\sum_{j=1}^{n}D_{ij}\left[\nabla x_j+\left(x_j-\omega_j\right)\frac{\nabla p}{p}\right]\right\}=0$
Energy conservation	$\rho_g\cdot C_{p,g}\cdot\vec{u}\cdot\nabla T+\nabla\cdot q=Q_h,\ \ q=-k_{eff}\nabla T$
	$Q_h=\frac{S_V iT\Delta S}{nF}+S_V i\left(\eta_{act}+\eta_{conc}\right)+\sum\frac{i^2}{\sigma_{eff}}$

Table 3 Material parameters [38, 39]

Parameter	Cathode	Electrolyte	Anode	Interconnect
Porosity, ε [38, 39]	0.4	–	0.4	–
Permeability, κ/m^2 [39]	1.76×10^{-11}	–	1.76×10^{-11}	–
Thermal conductivity, k/W·(m·K)$^{-1}$ [38, 39]	6	2.7	11	20
Heat capacity, C_p/J·(kg·K)$^{-1}$ [38, 39]	430	470	450	550

Table 4 Boundary conditions [35, 38, 39]

Boundary surface	Conditions
Fuel inlet	U_a=1, 2, 3, 4, 5 m/s [35]
	ω (H_2:H_2O)=0.4:0.6 [38, 39]
	T =923,973,1023,1073 [38, 39], 1123 K
Fuel outlet	P_0=0.1 MPa
Air inlet	U_c=1.5, 3 [38, 39], 4.5, 6, 7.5 m/s
	ω (O_2:N_2)=0.15:0.85 [38, 39]
	T=923,973,1023,1073 [38, 39], 1123 K
Air outlet	P_0=0.1 MPa
Side faces of the cell	Symmetric boundary conditions
Top and bottom surfaces	Periodic boundary condition (ΔT=0)

Table 5 Grid independence test

Mesh elements	Current density/A·m^{-2}	Relative error/%
Mesh1 (39 000)	4488.7	–
Mesh2 (60 000)	4538.7	1.11
Mesh3 (88 000)	4567.0	0.62
Mesh4 (100 800)	4578.4	0.24

Table 6 Meshing of computational domain

Dimension	Number of elements
Cathode thickness	4
Electrolyte thickness	4
Anode thickness	6
Gas channel width	20
Gas channel height	10
Interconnect width	10
Cell length	50

considered in this paper for subsequent research. The way of meshing in this study is shown in Fig. 1(a) and Table 6. Based on the range of potentials available in the experiment [38, 39], the model was verified in our previous study [41]. The simulation results show good agreement with the experimental data.

3. Results and Discussion

3.1 Effects of operating voltage

To investigate the effect of operating voltage on the thermal behavior of SOFC, simulations are performed in this section at an inlet gas temperature of 1073 K. At this time, the oxidant velocity is 3 m/s and the fuel velocity is 1 m/s. The operating voltage is varied from 0.9 V to 0.3 V. As expected, the current density increases from 1015.9 A/m^2 to 5799.0 A/m^2 when the voltage decreased from 0.9 V to 0.3 V. Meanwhile the peak power density of 2280.5 W/m^2 is reached at 0.6 V, as shown in Fig. 2(a). The electrochemical reaction rate varies under different operating voltages, which greatly influences the electrochemical reaction heats in SOFC. Here, three representative conditions with operating voltage values of 0.3 V, 0.6 V and 0.9 V are selected to analyze the thermal behavior inside the SOFC.

The heat source is mainly concentrated at the position where the electrolyte is in contact with the electrodes, and it gradually decreases away from the interfaces, as shown in Fig. 2. The distribution of heat source helps to understand the generation and distribution of heat. In comparison, more heat will be released at the anode-electrolyte interface, which is consistent with that described in Ref. [37]. As a key factor affecting the performance of the SOFC, the operating voltage is of great significance to the overall temperature characteristics of the cell. The variation of the operating voltage only affects the value of the maximum temperature, and would not change its position. The lower the operating voltage, the more the heat is generated, and the higher the overall temperature of the cell, as shown in Fig. 2(b). The combined effects of the electrochemical reaction heats, various overpotential losses and convective heat transfer efficiency are responsible for the above phenomenon and are discussed in detail below. The accumulation of electrochemical heat makes the SOFC temperature distribution uneven, which increases the temperature gradient in SOFC.

According to the literature [45], the region less than 10 K/cm is referred to as the safe zone in this study. Fig. 2(c) shows the axial temperature gradient distributions for the cases with different operation parameters. Each horizontal line represents the temperature gradient range at different axial locations for a fixed operation parameter. In the early study [31], there are four different ranges about temperature gradient: $|dT/dx| < 10$ K/cm, 10 K/cm $< |dT/dx| < 30$ K/cm, 30 K/cm $< |dT/dx| < 60$ K/cm, and $|dT/dx| > 60$ K/cm. The red lines are used to distinguish areas where the temperature gradient is less than 10 K/cm,

which represents the safe areas mentioned in the text. At 0.9 V, the temperature gradient is generally below 10 K/cm, which means that the temperature gradient is within safe limits throughout the SOFC. But the performance of the cell is low. As the operating voltage increases, a large temperature gradient value appears at the air inlet and extends to the middle region. At 0.3 V, although the current density is high, only about 20% of the area is in the safe temperature gradient range. Combining the Fig. 2(a) and Fig. 2(c), 0.6 V is a suitable operating voltage among our selection to ensure the power density of SOFC operation, but also to make SOFC have about 52% of the area in a safe temperature gradient range. Meanwhile, only about 8% of the area has a temperature gradient larger than 30 K/cm, which means that it has a good thermal performance [31]. In addition, the operating voltage also affects the gas distribution in SOFC. The lower the operating voltage is, the more the gas is consumed, and that is, the higher the utilization rate of the reactants. As the reaction proceeds, the oxygen molar concentration downstream of SOFC drops to a lower value rapidly, as shown in Fig. 2(d). In this case, the molar concentration of oxygen becomes a key factor affecting the performance of the cell. Therefore, this phenomenon should be avoided by reasonable flow field design and the selection of control parameters such as porosity and tortuosity.

As the operating voltage decreases, the net heat increases, as shown in Fig. 3(a). Various overpotential losses and anode heat generation account for a large proportion of the total heat source, which keeps the net heat positive. Generally, this is the main reason for the increase in temperature of SOFC. At operating voltage of 0.9 V, which means that SOFC is in a low current density state, since the negative reversible heat source at cathode is more than the sum of Joule heat and activation loss heat, the heat source at cathode contributes negatively to the heat generation of SOFC. As the operating voltage decreases, the net heat at cathode becomes positive, at which point the cathode also contributes to heat generation. The heat generation rate of each component of the SOFC varies under different operating voltages, as shown in Fig. 3(b). With the operating voltage variation, the share of net anode heat in the total heat gradually

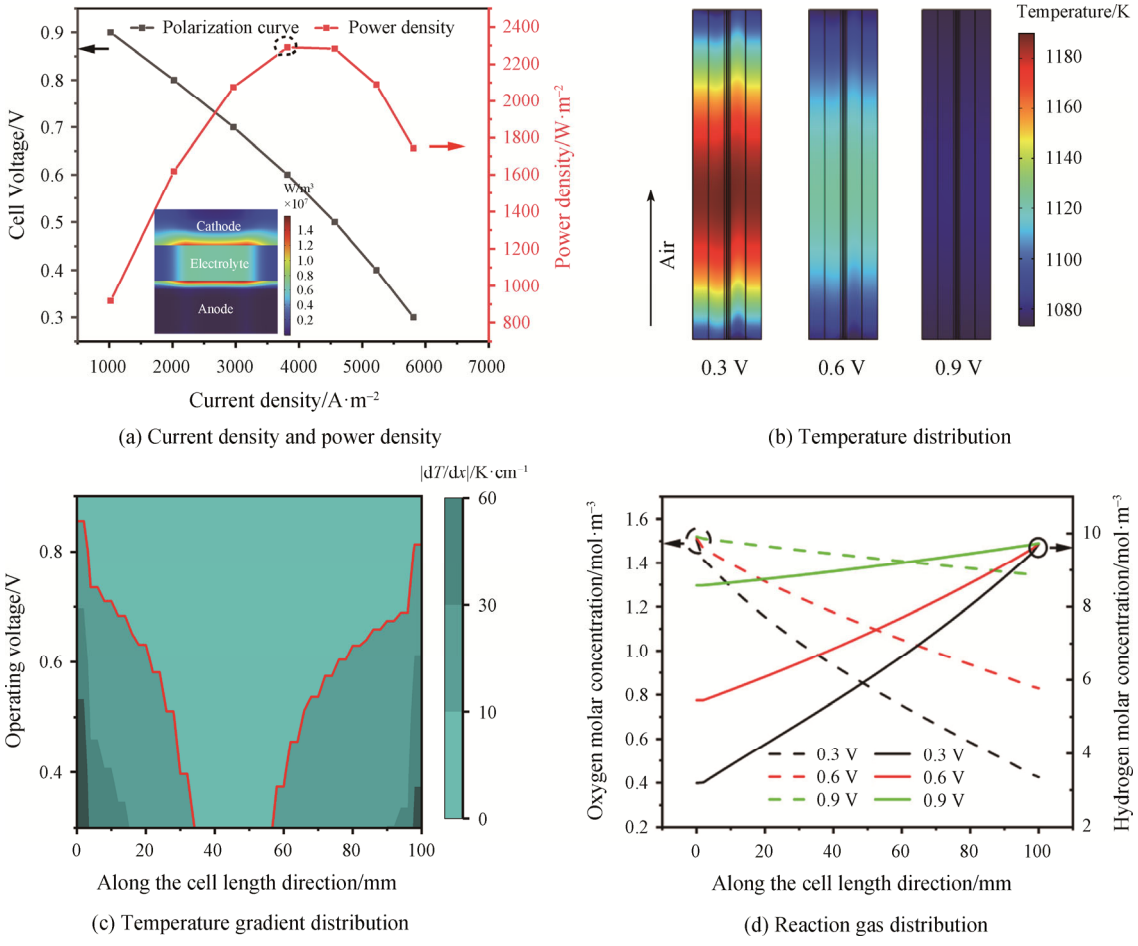

Fig. 2 Effects of the operating voltage

increases up to 75%. At the low voltage, ohmic heat also occupies a large proportion. The heat released from the anode is the key to control the SOFC temperature distribution. When the operating voltage drops from 0.6 V to 0.3 V, the net heat at anode increases by about 1.71 times, and the temperature increases by about 5.84%. Next, the thermal characteristics of the anode are analyzed. Along the length of the cell, the heat source decreases. A higher heat source exists at the air inlet, especially at low voltage, as shown in Fig. 3(c).

For the anode, the total heat generation rate increases as the voltage decreases, which generates more heat. The interconnector plays the role of heat distribution, which can quickly make the temperature of each component tend to be consistent. However, the heat generation rate and heat transfer rate of the anode always mismatch. Here, a positive heat transfer rate means that the anode transfer heat to other components, and a negative heat transfer rate means that other components transfer heat to the anode, as shown in Fig. 3(d). At anode, the heat transfer rate increases as the operating voltage decreases. At the middle and low voltage, excessive heat generation is always seen at anode in comparison with its heat transfer rate, so the temperature of the SOFC continues to rise, and this difference becomes bigger with the operating voltage decrease. More heat is generated by anode, but it is difficult to be transported out in time, resulting in local heat accumulation. Therefore, thermal management is especially problematic at high current density.

3.2 Effect of oxidant velocity at cathode

As mentioned above, the gas velocity at the cathode inlet affects the oxygen distribution and convective heat transfer in SOFC. In this section, simulations are performed at an operating voltage of 0.6 V, an inlet gas temperature of 1073 K, and a fuel velocity of 1 m/s. Meanwhile, the oxidant velocity varies from 1.5 m/s to 7.5 m/s with an interval of 1.5 m/s to analyze the thermal behavior. As the oxidant velocity increases, the current density increases, as shown in Fig. 4(a). At this time, the loss of pump power also increases, reducing the net power [10]. The oxidant velocity at cathode affects the gas concentration distribution under the flow channel and under the rib, as shown in Fig. 4(b). When velocity U_c is 1.5 m/s, the cathode is starved of oxygen at high current

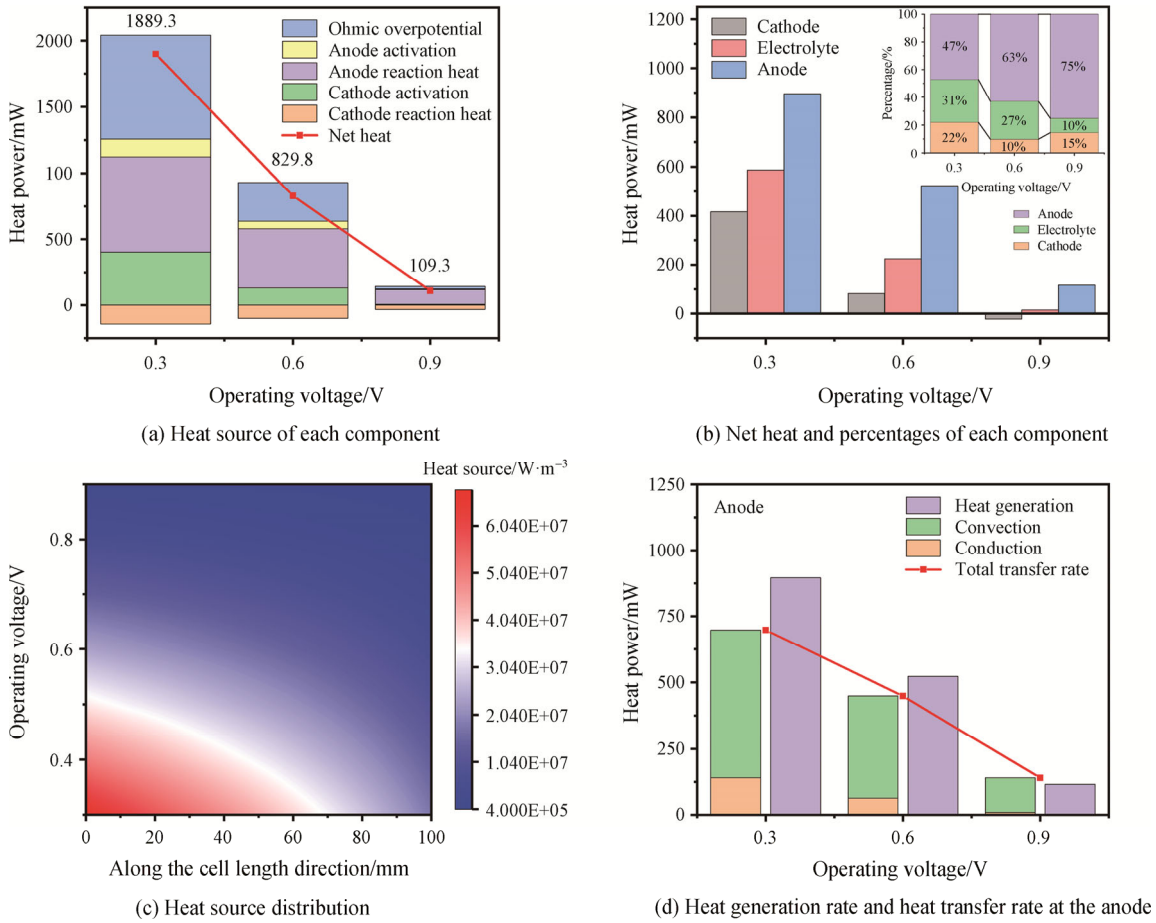

(a) Heat source of each component

(b) Net heat and percentages of each component

(c) Heat source distribution

(d) Heat generation rate and heat transfer rate at the anode

Fig. 3 Effects of the operating voltage

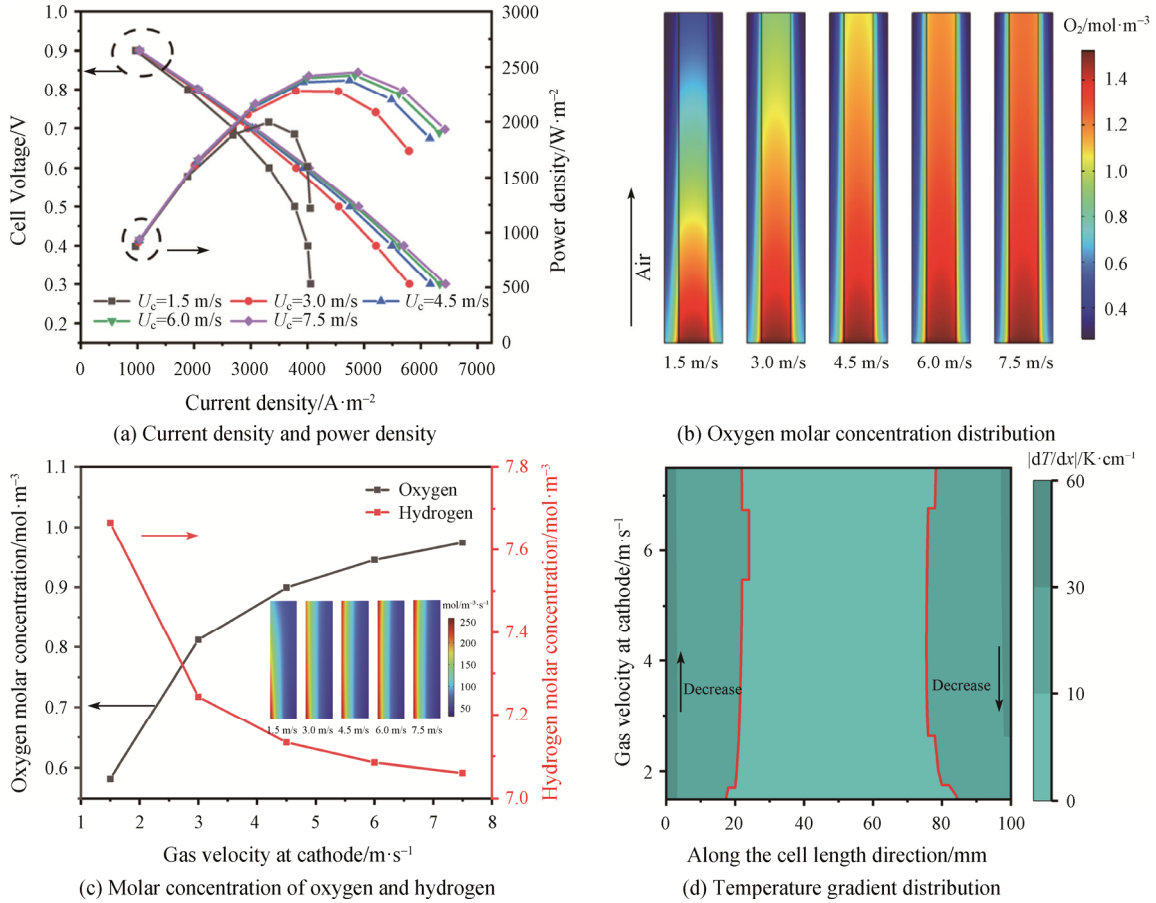

Fig. 4 Effects of the oxidant velocity

densities and the power density is drastically reduced. It can be seen that the electrochemical performance of the cell is mainly limited by the insufficient supply of oxygen in the reaction at the low oxidant velocity. This situation can be improved by increasing inlet velocities. The improvement of the oxidant velocity enhances the diffusion of oxygen, increases the average oxygen molar concentration, reduces the local low oxygen area, and enhances the electrochemical reaction. As the oxidant velocity increases, the molar concentration of hydrogen decreases due to the enhancement of the electrochemical reaction, as shown in Fig. 4(c). In addition, the reaction rate of oxygen is more uniform. When the oxidant velocity exceeds 3 m/s, there is a temperature gradient higher than 30 K/cm near the fuel inlet, which is likely to generate large thermal stresses and thus lead to cracks, as shown in Fig. 4(d). During the change of oxidant velocity, the trend of temperature gradient distribution of SOFC is basically constant. However, the peak temperature gradient near the air inlet decreases with increasing oxidant velocity, where 16.59% decrease in the maximum temperature gradient is observed.

The oxidant velocity has a large effect on the total heat source distribution, especially at low velocities, as shown in Fig. 5(a). It can be seen that the variation of the heat source depends on the reaction state. When the SOFC is in oxygen starvation, increasing the oxidant velocity results in a large increase for the heat source, with a 17.35% increase in the heat generation. The reaction heat in electrodes is increased due to the increase of oxidant velocity, as well as a decrease in the activation loss heat of the cathode. So, the contribution of the heat source at cathode becomes smaller during the change of oxidant velocity. Adequate oxygen further increases the net heat at anode, as shown Fig. 5(b). The maximum temperature of SOFC is influenced by the oxidant velocity. At low oxidant velocities, the downstream oxygen concentration is insufficient such that the heat source is concentrated at the air inlet, as shown in Fig. 5(c). The increase in oxidant velocity leads to an increase in the reaction rate, which means more heat generation and increases the temperature of SOFC. At the same time, the heat source contribution of anode is increasing and the net heat is rising. However, when velocity U_c exceeds 4.5 m/s, the maximum temperature decreases, as shown in Fig. 5(d). This is due to the fact that the maximum temperature is affected by a combination of both electrochemical reaction and convective heat transfer, and the decrease in

temperature represents a greater effect of convective heat transfer than electrochemical heat generation. The trend of net heat is the same as the trend of current density. When velocity U_c exceeds 4.5 m/s, the cell performance and the net heat improve by less than 3%, as shown in Fig. 4(a) and Fig. 5(a). The contribution of both thermal conduction and convective heat transfer increases as the oxidant velocity increases. However, excessive heat generation at anode in comparison with the heat transfer rate is always observed. The interconnector transports excess heat from the anode to the cathode, where the excess heat can be cooled by the air with high velocities, ultimately lowering the overall temperature of the SOFC.

3.3 Effect of fuel velocity at anode

In this section, simulations are performed at an operating voltage of 0.6 V, an inlet gas temperature of 1073 K, and an oxidant velocity of 3 m/s. The fuel velocity is changed in the range between 1 m/s and 5 m/s with an interval of 1 m/s [35] to analyze the thermal behavior. As the fuel velocity increases, the current density also increases, as shown in Fig. 6(a). However, the power density increase is very small, only 5%. Similarly, the pump power increases as the fuel velocity increases. During the change of fuel velocity, the overall temperature decreases, while the peak temperature moves towards the fuel outlet, as shown in Fig. 6(b). The above analysis shows that the anode is the key to regulate the temperature field of SOFC. The high fuel velocities in the anode channel results in better convective heat transfer, which leading to more uniform temperature distribution. Meanwhile, when velocity U_a exceeds 1 m/s, excessive heat transfer at anode in comparison with its heat generation, which is the reason for the drop in SOFC temperature. As the fuel velocity increases, the oxygen molar concentration gradually decreases, while the hydrogen molar concentration increases, as shown Fig. 6(c). The fuel velocity at anode has a large effect on the distribution of the temperature gradient, as shown Fig. 6(d). The maximum temperature gradient increases with the increase of fuel velocity, with a 21.2% increase. However, at high fuel flow velocities, there is a wider safety zone, which means that the increase in fuel velocity eliminates part of the high temperature gradient zone at the fuel inlet and reduces the danger-prone zone, with a 32% decrease.

The fuel velocity has a negligible effect on the total heat source distribution, as shown in Fig. 7(a). The

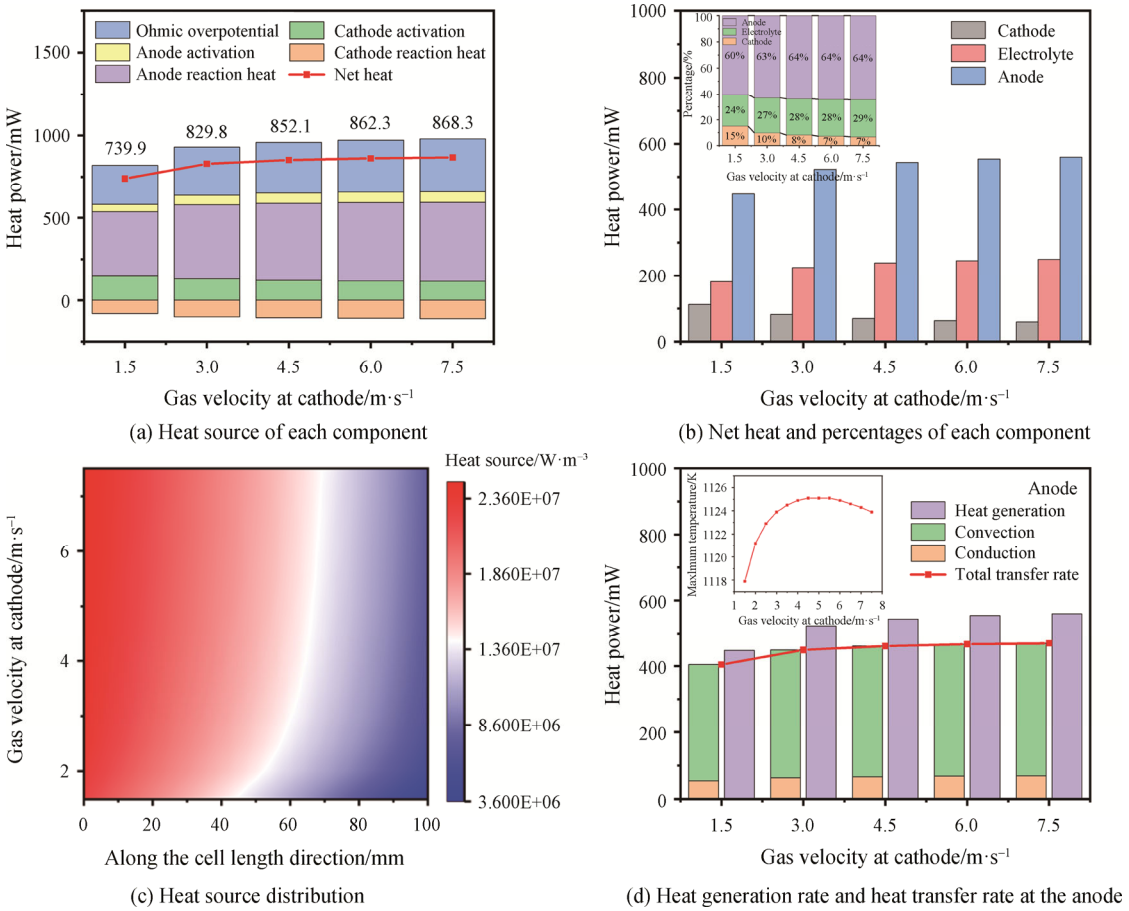

Fig. 5 Effects of the oxidant velocity

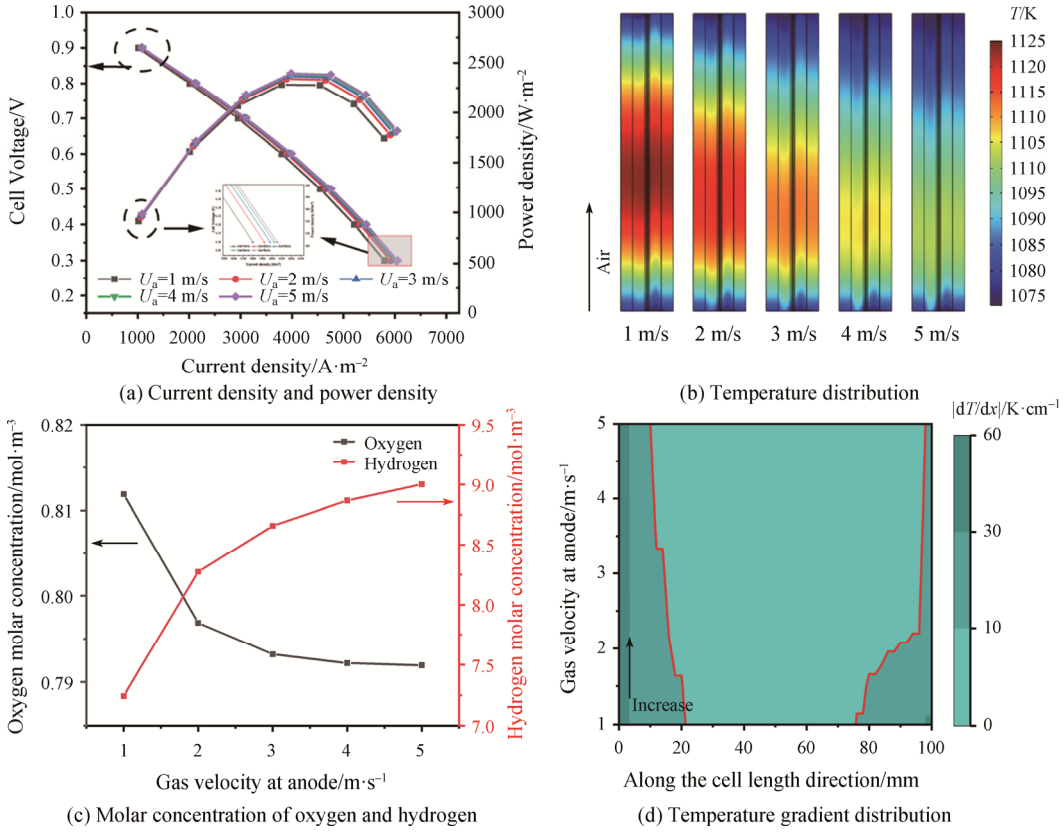

Fig. 6 Effects of the fuel velocity

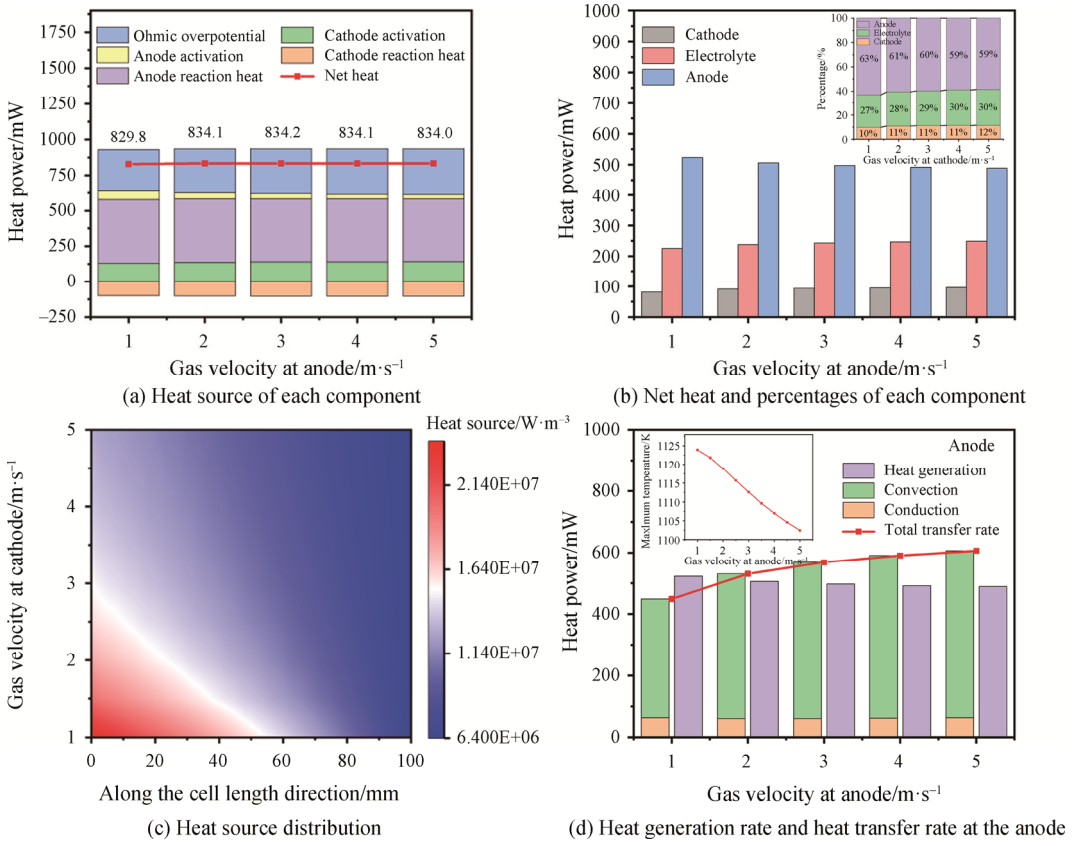

Fig. 7 Effects of the fuel velocity

decrease in the reaction heat source of the anode can overcome the increase in the heat source of the cathode and electrolyte. It is clear that the heat power is almost the same, which is in agreement with the trend of the current density. As the fuel velocity increases, the contribution of the heat source at anode becomes smaller. Meanwhile, the increase in fuel load with increasing inlet fuel flow makes the contribution of the cathode and electrolyte heat sources larger, as shown Fig. 7(b). During the change of fuel velocity, the heat source of air inlet is lowered and the high heat source region is gradually reduced, as shown in Fig. 7(c). It can be seen that contribution of convective heat transfer to the total heat transfer rate increases at anode, as shown in Fig. 7(d). However, thermal conduction is hardly influenced by variation in the fuel velocity. When velocity U_a exceeds 1 m/s, the heat transfer rate exceeds the heat generation rate. Interestingly, it is consistent with the decreasing trend of the maximum temperature. At higher fuel velocities, the difference between the heat transfer rate and the heat generation rate is greater, when the temperature drops by about 21.4 K. The key to regulate the temperature field of SOFC is to regulate the heat generation and consumption inside the anode so that the heat generation rate and heat transfer rate are balanced as much as possible, which is important for the temperature variation and distribution inside the SOFC.

3.4 Effects of reactant inlet temperature

The gas temperature at the inlet is a key factor affecting the kinetics of electrochemical reactions, which directly affects the generation of heat and the thermodynamic behavior. Here, simulations are performed at an operating voltage of 0.6 V, an oxidant velocity of 3 m/s, and a fuel velocity of 1 m/s, with inlet temperature varying from 923 K to 1123 K to analyze the thermal behavior.

As the inlet gas temperature increases, the ionic conductivity increases. Thus the current density is significantly increased, as shown in Fig. 8(a), which is consistent with the conclusion of the literature [46]. Due to the complex process of internal heat absorption and heat release, there is a huge difference between the inlet gas temperature and the maximum temperature of the cell.

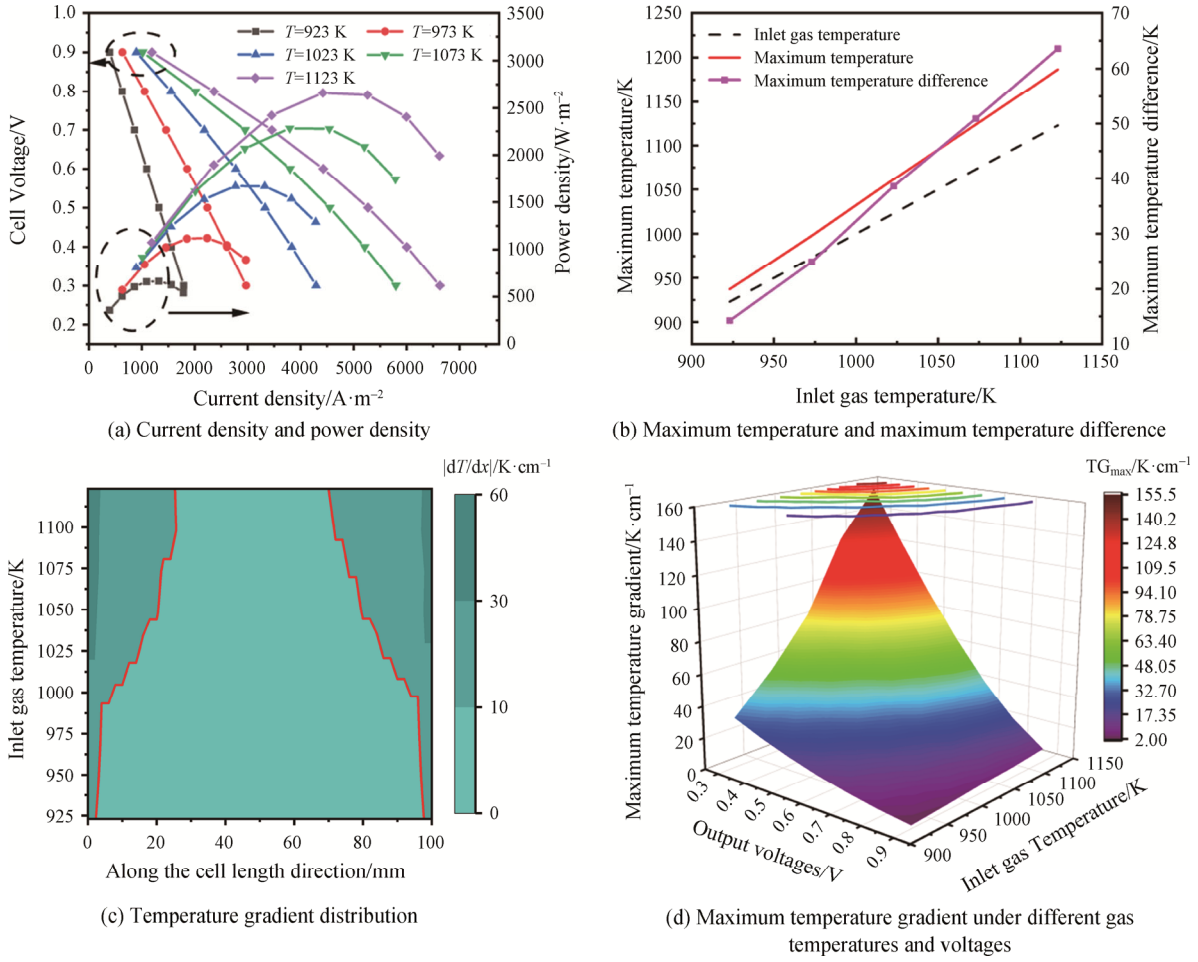

(a) Current density and power density

(b) Maximum temperature and maximum temperature difference

(c) Temperature gradient distribution

(d) Maximum temperature gradient under different gas temperatures and voltages

Fig. 8 Effects of the reactant inlet temperature

As the inlet temperature increases, the electrochemical reaction becomes more intense and more heat is generated. The maximum temperature difference of the cell rises, as shown in Fig. 8(b). When the inlet gas temperature is 1123 K, the maximum temperature difference inside the SOFC can be observed to be about 63 K. Although increasing the inlet gas temperature improves the electrochemical performance, it increases greatly the temperature gradient between the inlet and outlet and reduces the area with the safe temperature gradient, as shown in Fig. 8(c). It is harmful to the SOFC reliability. We can reduce the peak temperature gradient and increase the area of the safety zone by controlling the gas velocity. In addition, the effect of the inlet gas temperature and operating voltage on the distribution of the temperature gradient is consistent, as shown in Fig. 8(d). The lower the operating voltage, the higher the inlet gas temperature, and the higher the temperature gradient occurs in the SOFC.

The increase in the reactant inlet temperature leads to an increase in all heat sources, with the largest increase in the reversible heat source at anode. It is mainly caused by the entropy changes of the H_2 electrochemical reactions, indicating that more electrochemical reactions occurred. As the reactant inlet temperature drops from 1123 K to 923 K, the heat generation is reduced by about 75.29%, as shown in Fig. 9(a). As the reactant inlet temperature increases, the porous anode contributes more and more to the total heat, accounting for about 71% of the total heat source. It can be seen that the heat generation rate of the anode is more sensitive to the increase in temperature. Therefore, it can be inferred that the temperature of the inlet limits the heat generation rate of the anode. At higher inlet gas temperatures, excessive reversible heat source at cathode in comparison with the activation heat loss from cathode is observed, which can result in less net heat at cathode, as shown in Fig. 9(b). When the reactant inlet temperature is higher than 1023 K, there is a higher heat source at the air inlet, as shown in Fig. 9(c). Meanwhile, temperature gradients above 30 K/cm occur near the air inlet, which may form cracks and affect the working life of the SOFC, as shown in Fig. 8(c). As the reactant inlet temperature rises, the thermal conduction and convective heat transfer at anode also rises, as shown in Fig. 9(d). During the gas temperature variation, heat generation rate is more than heat transfer rate at anode, and the temperature of the SOFC continues to rise.

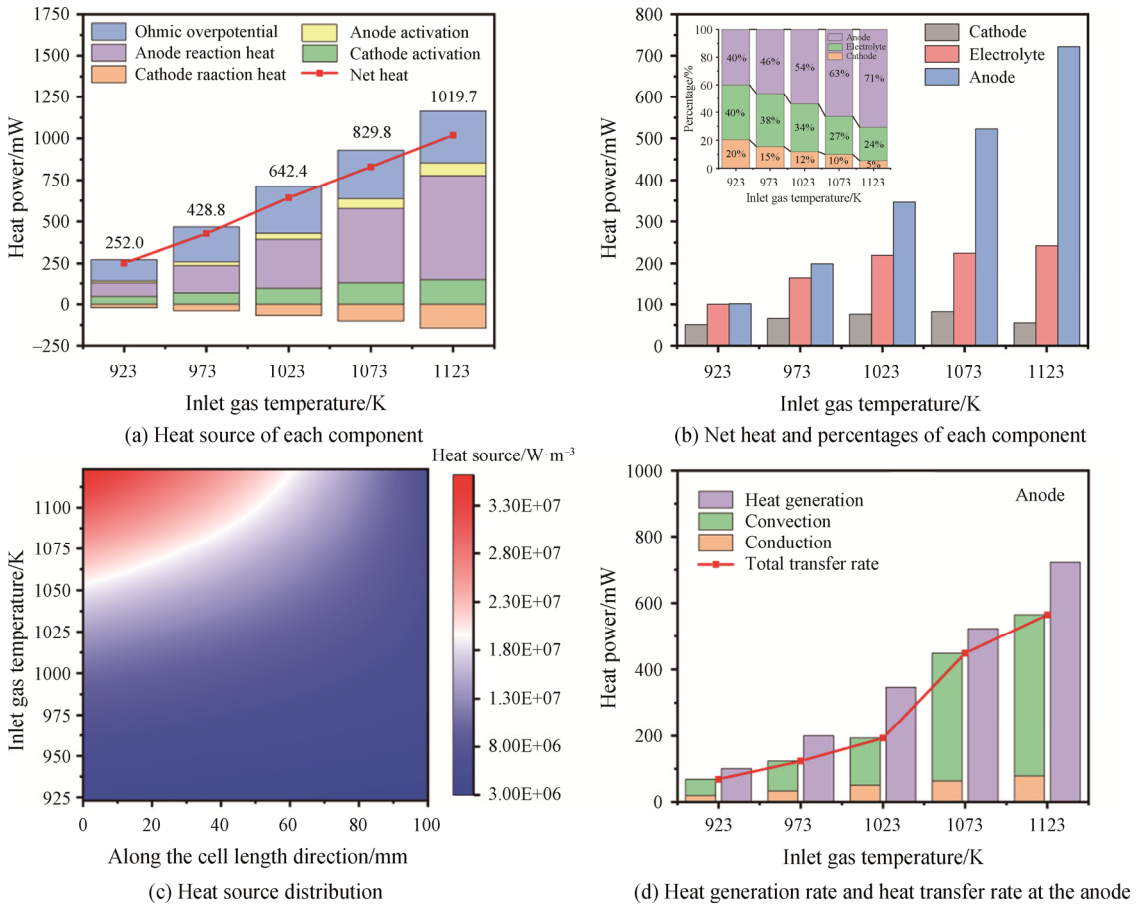

Fig. 9 Effects of the reactant inlet temperature

3.5 Effects of flow modes

The flow mode has an important influence on the temperature and temperature gradient distribution inside the SOFC. The highest temperature appears near the outlet under the mode of co-flow, and the temperature rises by about 89.8 K. While under the mode of counter-low, the SOFC shows a distribution trend of high temperature in the middle and low temperature on both sides. At this time, the maximum temperature difference is about 50.8 K, as shown in Fig. 10(a). Along the flow direction, the temperature gradient of the co-flow is lower, which occurs at the air inlet, and maintains a downward trend toward the outlet. At 0.6 V, a safe region of approximately 52% exists, making the SOFC temperature gradient less than 10 K/cm, as shown in Fig. 10(b). The counter-flow makes the overall temperature of the SOFC lower, but there are large temperature gradients at the gas inlet and outlet, which has a great impact on the long-term operation reliability of SOFC. The co-flow mode has a safer temperature gradient. The heat sources of each component along the flow direction are different. The heat sources at electrolyte and cathode are the same distribution trend. Specifically, the trend of counter-flow tends to increase along the air inlet, while the trend of co-flow tends to decrease along the air inlet, as shown in Fig. 10(c) and Fig. 10(d). Besides, in both flow modes, the anode heat source is elevated along the fuel inlet. The heat accumulation in the electrolyte is the largest under co-flow, while the most uniform heat source distribution in the electrolyte is under counter-flow. It is also worth noting that the higher the current density is not always corresponding to the higher maximum temperature of SOFC. The temperature of the cell is controlled by the combining function of both the degree of electrochemical reaction and the efficiency of convective heat transfer. In comparison, current density is generally higher under the mode of counter-flow. However, the maximum temperature under counter-flow is 39 K lower than that under co-flow, and the maximum temperature gradient is about 32 K/cm higher than that under co-flow. When choosing the flow mode, it is necessary to consider both the maximum temperature and the temperature gradient to avoid large thermal stress.

For different flow modes, there is no significant difference in the heat generation rate at anode. The greater difference is in the heat transfer rate. And the heat transfer rate for the co-flow is higher. But in both cases, the heat transfer rate is smaller than the heat generation

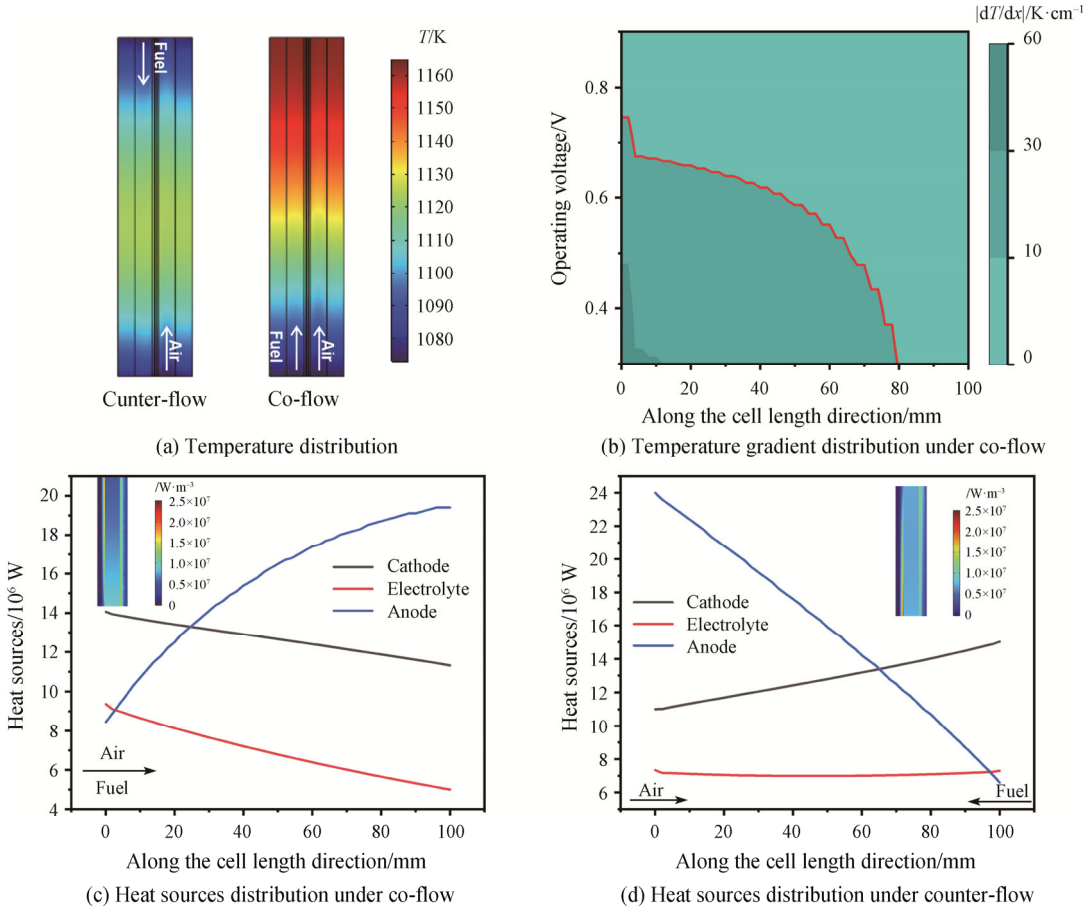

Fig. 10 Effects of the flow modes

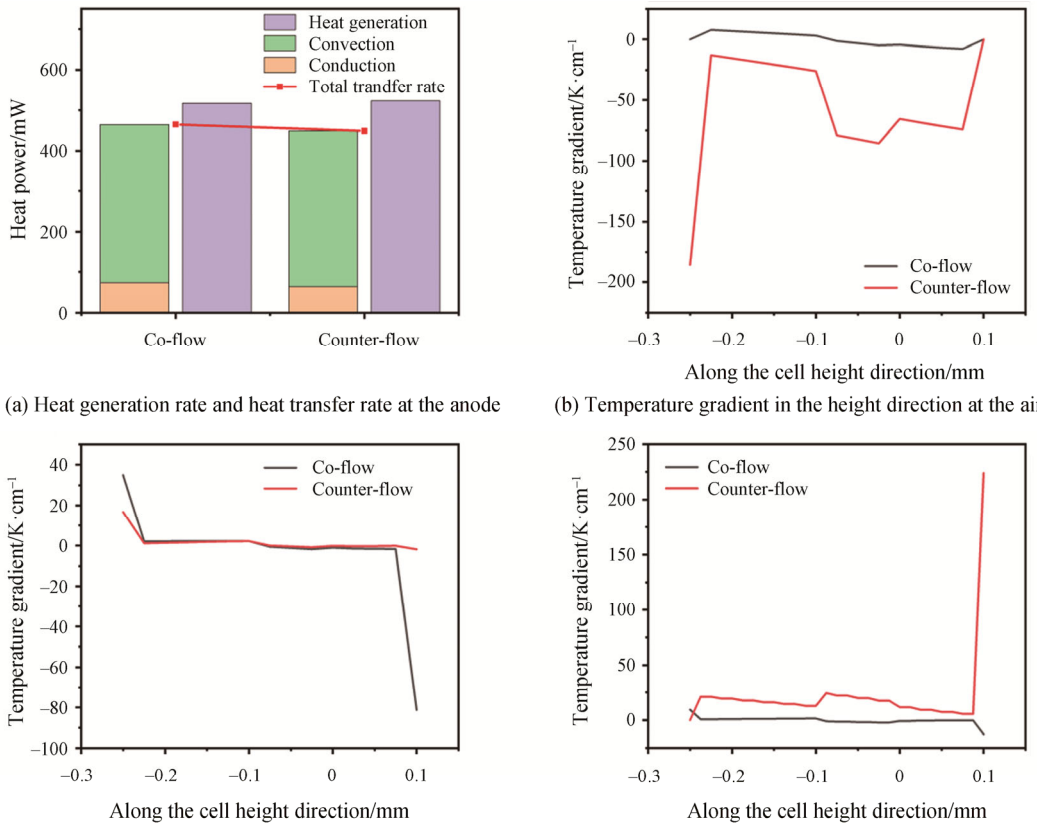

(a) Heat generation rate and heat transfer rate at the anode

(b) Temperature gradient in the height direction at the air inlet

(c) Temperature gradient in the height direction of the middle section

(d) Temperature gradient in the height direction at the air outlet

Fig. 11 Effects of the flow modes

rate, as shown in Fig. 11(a). The temperature change in SOFC is mainly reflected in the direction of flow, and the change of thermal parameters in the height direction was ignored in many studies. The temperature gradient distribution of the two flow modes at the air inlet is a large difference, as shown in Fig. 11(b). Under counter-flow, a large temperature gradient is observed at the interface of anode and fuel at the air inlet, approximately –186.0 K/cm. This may be due to the higher heat accumulation. The temperature gradient in the middle section is closer; at the position where the cathode is in contact with the air, there is a large temperature gradient under the co-flow, as high as –81.3 K/cm, as shown in Fig. 11(c). The temperature gradient distribution at the air outlet is consistent. At the position where the cathode is in contact with the air, there is a large temperature gradient under the counter-flow, as high as 224.0 K/cm, as shown in Fig. 11(d). This may be due to the strongest convective heat transfer effect of the air at this position, so it can fully dissipate heat, and then form a large temperature gradient.

4. Conclusions

A three-dimensional multi-physics numerical model for a planar SOFC was built and its accuracy was verified. The thermal behavior of SOFC under different operation conditions was discussed. The effects of the operation conditions on the heat generation rate and heat transfer rate at anode were analyzed.

Parametric studies show that the electrochemical reaction heat, various overpotential losses and convective heat transfer efficiency together affect the temperature distribution in SOFC, and temperature distribution is affected generally by adjusting the gas velocity. For the studied case, increasing the fuel velocity decreases the temperature of SOFC by up to 21.4 K. At high fuel velocities, a 32% reduction in the danger zone is achieved, but the peak temperature gradient increases at the air inlet by about 21.2%. However, at high oxidant velocities, a 16.59% decrease in the maximum temperature gradient is observed. High heat sources generally occur at high oxidant velocities as well as low fuel velocities.

The maximum temperature gradient is affected by the synergistic effect of the operating voltage and the inlet gas temperature. At low voltages and high inlet temperatures, the SOFC has a small safety zone. Meanwhile, a higher heat source exists at the air inlet. The heat generation rate at anode is more sensitive to the increase in temperature, accounting for about 71% of the total heat source. This means that the porous anode is the

main heat generation site and its heat release is the key to control the SOFC temperature distribution.

The temperature varies mainly along the flow direction. However, the thermal characteristics in the height direction cannot be ignored. Attention should be paid on the location of large temperature gradients in the height direction, such as the cathode-air interface and the anode-fuel interface at the air inlet and outlet under counter-flow, and the cathode-air interface at the middle section under co-flow.

This study provides a certain reference for the research on the thermal effect and temperature gradient distribution of the cell, emphasizing that the importance of high fuel velocities in reducing the areas where the temperature gradient exceeds the limits, which comes at the cost of the loss of pump power. Effectively balancing the gain of increasing the safety zone and the loss of pump power is the key for subsequent research.

Acknowledgements

The authors are grateful for the supports provided by the Science and Technology Research Program of Henan Province, China (No. 222102320230) and the National Natural Science Foundation of China (No. 51776190).

Conflict of Interest

On behalf of all authors, the corresponding author states that there is no conflict of interest.

References

[1] Li D.D., Zhao H.X., Kong F.C., et al., Application of ejector in solid oxide fuel cell anode circulation system. Journal of Thermal Science, 2022, 31(3): 634–649.

[2] Zeng Z.Z., Qian Y.P., Zhang Y.J., et al., A review of heat transfer and thermal management methods for temperature gradient reduction in solid oxide fuel cell (SOFC) stacks. Applied Energy, 2020, 280: 115899.

[3] Deng M.L., Liu J.Y., Zhang X.S., et al., Energy and parameter analysis of SOFC system for hydrogen production from methane steam reforming. Journal of Thermal Science, 2022, 31(6): 2088–2110.

[4] Patcharavorachot Y., Arpornwichanop A., Chuachuensuk A., Electrochemical study of a planar solid oxide fuel cell: Role of support structures. Journal of Power Sources, 2008, 177(2): 254–261.

[5] Raj A., Sasmito A.P., Shamim T., Numerical investigation of the effect of operating parameters on a planar solid oxide fuel cell. Energy Conversion and Management, 2015, 90: 138–145.

[6] Wang Y., Zhan R.B., Qin Y.Z., et al., Three-dimensional modeling of pressure effect on operating characteristics and performance of solid oxide fuel cell. International Journal of Hydrogen Energy, 2018, 43(43): 20059–20076.

[7] Fu P., Yang J., Wang Q.W., Numerical study on mass transfer and electrical performance of anode-supported planar solid oxide fuel cells with gradient porosity anode. Journal of Heat Transfer, 2020, 142(2): 022101.

[8] Zhang X.Q., Espinoza M., Li T.S., et al., Parametric study for electrode microstructure influence on SOFC performance. International Journal of Hydrogen Energy, 2021, 46(75): 37440–37459.

[9] Danilov V. A., Tade M. O., A CFD-based model of a planar SOFC for anode flow field design. International Journal of Hydrogen Energy, 2009, 34(21): 8998–9006.

[10] Zhan R.B., Wang Y., Ni M., et al., Three-dimensional simulation of solid oxide fuel cell with metal foam as cathode flow distributor. International Journal of Hydrogen Energy, 2020, 45(11): 6897–6911.

[11] Wang Y.Q., Chen J.S., Liu K.L., et al., Computational screening of La_2NiO_4+delta cathodes with Ni site doping for solid oxide fuel cells. Inorganic Chemistry, 2023, 62(19): 7574–7583.

[12] Hao C.K., Zeng Z.Z., Zhao B.G., et al., Local heat generation management for temperature gradient reduction in tubular solid oxide fuel cells. Applied Thermal Engineering, 2022, 211: 118453.

[13] Fan P.F., Li G.J., Zeng Y.K., et al., Numerical study on thermal stresses of a planar solid oxide fuel cell. International Journal of Thermal Sciences, 2014, 77: 1–10.

[14] Xu M., Li T. S., Yang M., et al., Modeling of an anode supported solid oxide fuel cell focusing on thermal stresses. International Journal of Hydrogen Energy, 2016, 41(33): 14927–14940.

[15] Shao Q., Bouhala L., Fiorelli D., et al., Influence of fluid flow and heat transfer on crack propagation in SOFC multi-layered like material with anisotropic porous layers. International Journal of Solids and Structures, 2016, 78–79: 189–198.

[16] Shao Q., Fernández-González R., Ruiz-Morales J.C., et al., An advanced numerical model for energy conversion and crack growth predictions in solid oxide fuel cell units. International Journal of Hydrogen Energy, 2015, 40(46): 16509–16520.

[17] Luo Y., Jiang W.C., Zhang Q., et al., Effects of anode porosity on thermal stress and failure probability of planar solid oxide fuel cell with bonded compliant seal. International Journal of Hydrogen Energy, 2016, 41(18): 7464–7474.

[18] Fang X.R., Lin Z.J., Numerical study on the mechanical stress and mechanical failure of planar solid oxide fuel

cell. Applied Energy, 2018, 229: 63–68.

[19] Wu Y.Y., Shi Y.X., Cai N.S., et al., Thermal modeling and management of solid oxide fuel cells operating with internally reformed methane. Journal of Thermal Science, 2018, 27(3): 203–212.

[20] Serincan M.F., Pasaogullari U., Singh P., Controlling reformation rate for a more uniform temperature distribution in an internal methane steam reforming solid oxide fuel cell. Journal of Power Sources, 2020, 468: 228310.

[21] Zhang Z.Q., Wang Y.L., Ba L., Analysis of heat and mass transfer for a single-planar-anode-supported solid oxide fuel cell considering internal reforming. Journal of Thermal Science, 2019, 29(3): 697–707.

[22] Huang C.M., Shy S.S., Lee C.H., On flow uniformity in various interconnects and its influence to cell performance of planar SOFC. Journal of Power Sources, 2008, 183(1): 205–213.

[23] Ramírez-Minguela J.J., Alfaro-Ayala J.A., Rangel-Hernández V.H., et al., Numerical analysis of the effect of trapezoidal baffles inside fuel and air channels on the performance of a planar-type solid oxide fuel cell. Journal of Thermal Science and Engineering Applications, 2022, 14(4): 041004.

[24] Lee H.M., Yuan P., Liu S.F., Thermal and electrical analysis in a solid oxide fuel cell stack using a curved profile for the inlet flow rate along the stacking direction. International Journal of Green Energy, 2014, 12(2): 117–124.

[25] Yuan P., Liu S.F., Effect of non-uniform inlet flow rate on the heat-up process of a solid oxide fuel cell unit with cross-flow configuration. International Journal of Hydrogen Energy, 2016, 41(28): 12377–12386.

[26] Zhang Z.G., Yue D.T., Yang G.G., et al., Three-dimensional CFD modeling of transport phenomena in multi-channel anode-supported planar SOFCs. International Journal of Heat and Mass Transfer, 2015, 84: 942–954.

[27] Choudhary T., Sanjay, Computational analysis of IR-SOFC: Thermodynamic, electrochemical process and flow configuration dependency. International Journal of Hydrogen Energy, 2016, 41(2): 1259–1271.

[28] Lee S., Kim H., Yoon K.J., et al., The effect of fuel utilization on heat and mass transfer within solid oxide fuel cells examined by three-dimensional numerical simulations. International Journal of Heat and Mass Transfer, 2016, 97: 77–93.

[29] Kim D.H., Bae Y., Lee S., et al., Thermal analysis of a 1-kW hydrogen-fueled solid oxide fuel cell stack by three-dimensional numerical simulation. Energy Conversion and Management, 2020, 222: 113213.

[30] Zheng K.Q., Sun Y., Shen S.L., et al., A novel cooler for the thermal management of solid oxide fuel cell stack. Sustainable Energy Technologies and Assessments, 2021, 48: 101564.

[31] Zeng Z.Z., Hao C.K., Zhao B.G., et al., Local heat transfer enhancement by recirculation flows for temperature gradient reduction in a tubular SOFC. International Journal of Green Energy, 2021, 19(10): 1132–1147.

[32] Xu H.R., Ma J.B., Tan P., et al., Towards online optimisation of solid oxide fuel cell performance: Combining deep learning with multi-physics simulation. Energy and AI, 2020, 1: 100003.

[33] Wang C., He Q.J., Li Z., et al., Modelling of solid oxide fuel cells with internal glycerol steam reforming. International Journal of Hydrogen Energy, 2022, 47(33): 15012–15023.

[34] Aman N.A.M.N., Muchtar A., Rosli M.I., et al., Influence of thermal conductivity on the thermal behavior of intermediate-temperature solid oxide fuel cells. Journal of Electrochemical Science and Technology, 2020, 11(2): 132–139.

[35] Shen Q.W., Li S.A., Yang G.G., et al., Analysis of heat and mass transport characteristics in anode-supported solid oxide fuel cells at various operating conditions. Numerical Heat Transfer, Part A: Applications, 2019, 75(8): 509–522.

[36] Xu Q.D., Xia L.C., He Q.J., et al., Thermo-electrochemical modelling of high temperature methanol-fuelled solid oxide fuel cells. Applied Energy, 2021, 291: 116832.

[37] Lee S., Park M., Kim H., et al., Thermal conditions and heat transfer characteristics of high-temperature solid oxide fuel cells investigated by three-dimensional numerical simulations. Energy, 2017, 120: 293–305.

[38] Khazaee I., Rava A., Numerical simulation of the performance of solid oxide fuel cell with different flow channel geometries. Energy, 2017, 119: 235–244.

[39] Park J., Kim D., Baek J., et al., Effect of electrolyte thickness on electrochemical reactions and thermo-fluidic characteristics inside a SOFC unit cell. Energies, 2018, 11(3): 473–487.

[40] Daun K.J., Beale S.B., Liu F., et al., Radiation heat transfer in planar SOFC electrolytes. Journal of Power Sources, 2006, 157(1): 302–310.

[41] Wang M.Y., Wang K., Wang Y.Q., et al., Analysis of mass transfer characteristics in a planar solid oxide fuel cell with a chaotic flow channel. Journal of Electroanalytical Chemistry, 2024, 956: 118071.

[42] Celik A.N., Three-dimensional multiphysics model of a planar solid oxide fuel cell using computational fluid dynamics approach. International Journal of Hydrogen Energy, 2018, 43(42): 19730–19748.

[43] Kakac S., Pramuanjaroenkij A., Zhou X.Y., A review of numerical modeling of solid oxide fuel cells. International Journal of Hydrogen Energy, 2007, 32(7): 761–786.

[44] Hafsia A., Bariza Z., Djamel H., et al., SOFC fuel cell heat production: Analysis. Energy Procedia, 2011, 6: 643–650.

[45] Aguiar P., Adjiman C.S., Brandon N. P., Anode-supported intermediate-temperature direct internal reforming solid oxide fuel cell. Journal of Power Sources, 2005, 147: 136–147.

[46] Wang Y.Q., Li X.C., Guo Z.N., et al., Effect of the reactant transportation on performance of a planar solid oxide fuel cell. Energies, 2021, 14(4): 1212–1225.